Chapter@6

Effect of sulfonated graphene on polyurethane properties

6.1 Introduction:

Blocky polyurethane elastomer is extensively used in biomedical area due to its biocompatible and versatile nature [Ganta et al. (2003)]. It is synthesized by a polyol such as polyether or / polyester, a diisocyanate and chain extender. Polyurethane contains urethane moiety in their chain and properties of these polymeric material can be modified by changing the chemical composition, nature and ratio of material used in synthesis process. Properties of polymer can also tune by incorporating the suitable nanofiller in matrix. Polymer with polyether polyol show the greater enzymatic degradation resistance than polyester based material and extensively used in preparation of medical scaffold for a long time application [da Silva et al. (2010)]. In recent year polymeric materials are extensively used in fuel cell application due to high energy conversation, low greenhouse effect and high power density over to the fossils fuel but due to the lack of aqueous solubility and electrical conductivity some modification is required to overcome these problems [Che et al. (2015); Wang et al. (2015)]. Dispersion of polyurethane in aqueous medium can be achieved by inserting the polar group such carboxylate or sulfonate moieties in their polymer chain which also facilitates the electrical conductivity of polyurethane [Williams et al. (2008)]. These grafted ions in polyurethane created an alternative possible to use in gel electrolyte in place of PVDF and its copolymer [Kim et al. (2013); Tsurumaki et al. (2015)]. Among various fuel cells proton exchange membrane fuel cell (PEMFC) has drawn the tremendous attention due to its high efficiency as well as minimum environmental impact [Wang et al. (2012); Steele et al. (2012); Wang et al. (2004)], but due the rapid performance loss restrict it for commercial applications. This problem can

be resolved by utilizing the stable carbon based nanomaterial. Among various carbon nanomaterials (fullerenes and carbon nanotubes) graphite has drawn the tremendous attention due to its extraordinary mechanical, thermal and electrical properties [Shen et al. (2012)], But due to inert and hydrophobic nature of graphite restrict it to use as metal nanocatalyst support materials [Park et al. (2009); Wang et al. (2008)]. Oxidation of graphite improves it hydrophilicity nature and reactivity which facilitated the good dispersion in aqueous medium as well as deposition on metal surface. However, loss in conductivity is occurred due to the defect which disturbs the conjugating structure of graphite [He et al. (2012); Xie et al. (2009)]. Conductivity can be achieved by reducing the graphene oxide by various reducing agents like hydrazine, sodium borohydrate etc. Sulfonation of graphene oxide by sulfonating agent cause the insertion of hydrophilic group as well as simultaneous reduction which improve the hydrophilic property and conductivity respectively [He et al. (2014)]. This sulfonated moiety facilitated the better deposition on metal surface which improve the overall performance.

In this article we have modified the graphene oxide into the sulfonated graphene oxide followed by the insertion of amine moiety in sulfonated graphene and evaluate the effect of this modified graphene on polyurethane property. Surface functionalization of graphene oxide is confirmed through FTIR, UV-visible, XRD and ^{1}H-NMR measurement. Different wt% of polyurethane functionalized graphene nanocomposites were prepared by chemically grafting the amine group of modified graphene with prepolymer chains. Homogenous dispersion was observed which is the key factor for the improvement in various properties of nanocomposites as compared to

pure polymer due to better interaction between polymer matrix and functionalized graphene sheet. Self-assembly phenomena are also facilitated in presence of functionalized graphene through the higher interaction. Nanocomposites exhibit the better corrosive resistance behavior indicating the developed materials may have the potential to utilize as corrosion resistance.

6.2 Results and Discussion:

6.2.1 FTIR and UV-visible spectra:

FTIR spectra of sulfonated graphene oxide followed by the functionalization through amine moiety are given in (Figure 6.1a). Appearance of the peaks at 1152 and 1077 cm^{-1} are associated to S=O stretching vibration indicating the presence of sulfonic moiety in modified graphene [He et al. (2014)]. Attenuated in peak intensity of carbonyl group (C=O, 1739 cm-1) indicates the simultaneous reduction process during sulfonation. Amine functionalization was done as reported by Lai et al. (2011). Appearance of absorption peak at 1575 cm^{-1} clearly indicates the presence of–(N-H) moiety in ring. Disappearance of the absorption peaks at 1398 cm^{-1}(C-OH) and 1739 cm^{-1} (-C=O) indicates the considerable de-hydration as well as de-carboxylation was occurred during the amine functionalization. UV-visible spectra of sulfonated followed by amine functionalized graphene is given in (Figure 6.1b). Pure graphene oxide was exhibited two absorption peak at 235 and 260nm for $\pi \rightarrow \pi^*$ and $n \rightarrow \pi^*$ respectively [Ma et al. (2012)]. For sulfonated graphene and sulfonated graphene with amine moiety this peak was shifted to 252nm and 255 nm respectively indicating the reduction of

graphene oxide and reformation of graphene electronic configuration as observed in FTIR spectra [Paredes et al. (2008)].

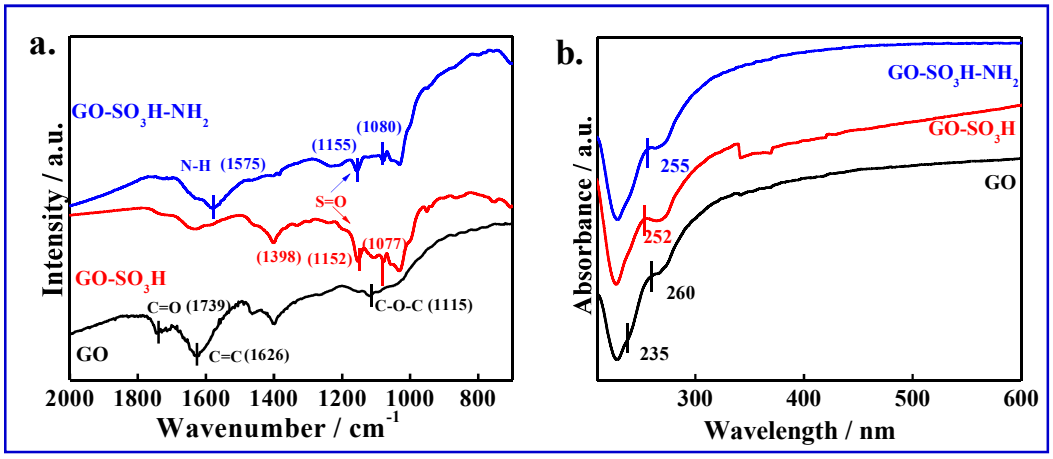

Figure 6.1: (a) FTIR and **(b)** UV-visible spectra of graphene oxide and modified graphene oxide.

6.2.2 XRD and ^{1}H-NMR of graphene oxide and modified graphene:

XRD pattern of graphene oxide and modified graphene oxide is given in (Figure 6.2a). Graphene oxide exhibits two diffraction peaks at 10.6^{0} (001) by insertion of oxygenated groups in ring and 24.7^{0} (002) graphitic sheet structure with corresponding d-spacing of 0.84nm and 0.37 nm respectively [Liu et al. (2012)]. After sulfonation very weak peak at 14.6^{0} with decreasing d-spacing from 0.84→0.61nm indicating the removal of some oxygenated moiety during the sulfonation. Another very broad diffraction peak with centered at 24.9^{0} corresponding d-spacing of 0.36 nm suggesting the reduction of graphene oxide [Fan et al. (2008)]. However, disappearance of peak at 14.6^{0} in sulfonated graphene with amine moiety and other very broad peaks at centered 24.9^{0} indicating the reduction of modified graphene oxide towards the graphitic

structure which is also verified through the FTIR and UV-visible spectra. ^{1}H-NMR spectra of graphene oxide and modified graphene oxide is given in (Figure 6.2b). ^{1}H-NMR lines in graphene oxide at 7.6 and 4.4ppm which is chemical shift of aromatic naphthelic hydrogen and hydroxyl group [Lai et al. (2011)]. Appearance of peak line at 8.9ppm in sulfonated graphene oxide indicates the presence of proton of sulfonyl group. Disappearance of peak line at 4.4ppm in sulfonated graphene indicates the dehydration process during the sulfonation.

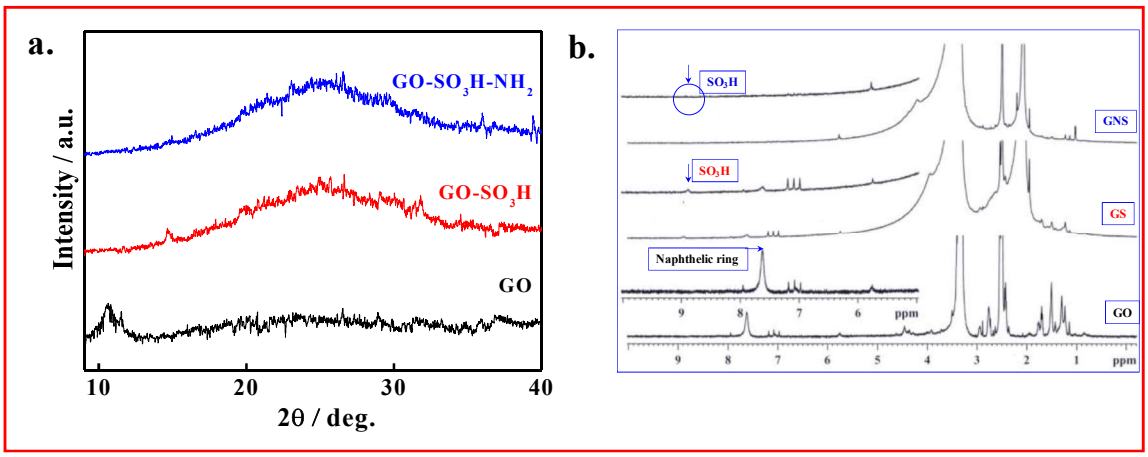

Figure 6.2: (a) XRD and **(b)** ^{1}H-NMR spectra of graphene oxide and modified graphene oxide.

6.2.3 Grafting of prepolymer chain to modified graphene:

Grafting of the prepolymer chain through the modified graphene is confirmed through ^{1}H-NMR measurement. ^{1}H-NMR spectra of pure polyurethane and its nanocomposites is given in (Figure 6.3). Pure polyurethane and nanocomposites exhibit a NMR line at ~7.0ppm indicating the presence of –(N-H) moiety of urethane linkage

while this peak intensity was reduced in nanocomposites due to the utilization of –NCO moiety of prepolymer chain to modified graphene [Mishra et al. (2010)]. Appearances of new peak in lower field region at~8.2ppm in nanocomposites clearly indicate the grafting of prepolymer chain to modified graphene [Patel et al. (2016)]. However, peak at ~9.8ppm in nanocomposites suggesting presence of SO_3H moiety which intensity becomes dominant in higher content of modified graphene.

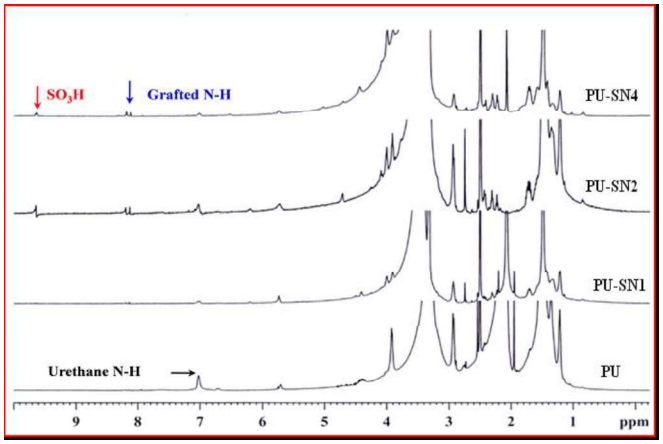

Figure 6.3: ^{1}H-NMR spectra of pure polyurethane and indicated nanocomposites.

6.2.4 Dispersion and Interaction:

Properties of material is highly depends upon the dispersion nature of nanofiller into matrix. Dispersion of functionalized graphene into polyurethane matrix is observed through TEM bright field images (Figure 6.4a). Homogenous dispersion was observed in nanocomposites even at higher content of the functionalized graphene which significantly influence the properties of nanocomposites through interaction. FTIR spectra of pure polyurethane and its indicated nanocomposites are given in (Figure 6.4b). Pure polyurethane exhibits a stretching peak at 3316 cm^{-1} for >N-H moiety

which shifted towards the higher wavenumber 3329 cm^{-1} in nanocomposites suggesting the strong interaction between the modified graphene sheet and polymer chains. Pure polyurethane exhibits strong absorption peak at ~1681 cm^{-1} and weak peak at ~1717 cm^{-1} indicating the presence of hydrogen bonded and free >C=O moiety in polymer chain [Kim et al. (2010)]. However, intensity of hydrogen bonded >C=O moiety was reduced and shifted towards higher frequency region 1684 cm^{-1} in nanocomposites indicate the greater interaction between polymer chain and modified graphene sheet. Whereas, intensity of free >C=O moiety becomes prominent in nanocomposites further suggesting the minimization of the interaction between urethane moiety and increasing the interaction between graphene sheet and polymer chains [Patel et al. (2015)]. Interaction between polymer chain and graphene sheet is also verified through UV-visible spectra and given in (Figure 6.4c). Pure polyurethane was exhibited two absorption peak at 250nm and 285nm for $\pi \rightarrow \pi^*$ and $n \rightarrow \pi^*$ respectively [Patel et al. (2016)]. Further prominent red shifting of $\pi \rightarrow \pi^*$ and $n \rightarrow \pi^*$ from 250→256nm and 285→293nm in nanocomposites also confirmed the good interaction with polymer chain possibly through dipolar interaction between the electronic moiety of modified graphene sheet and urethane moiety of polyurethane.

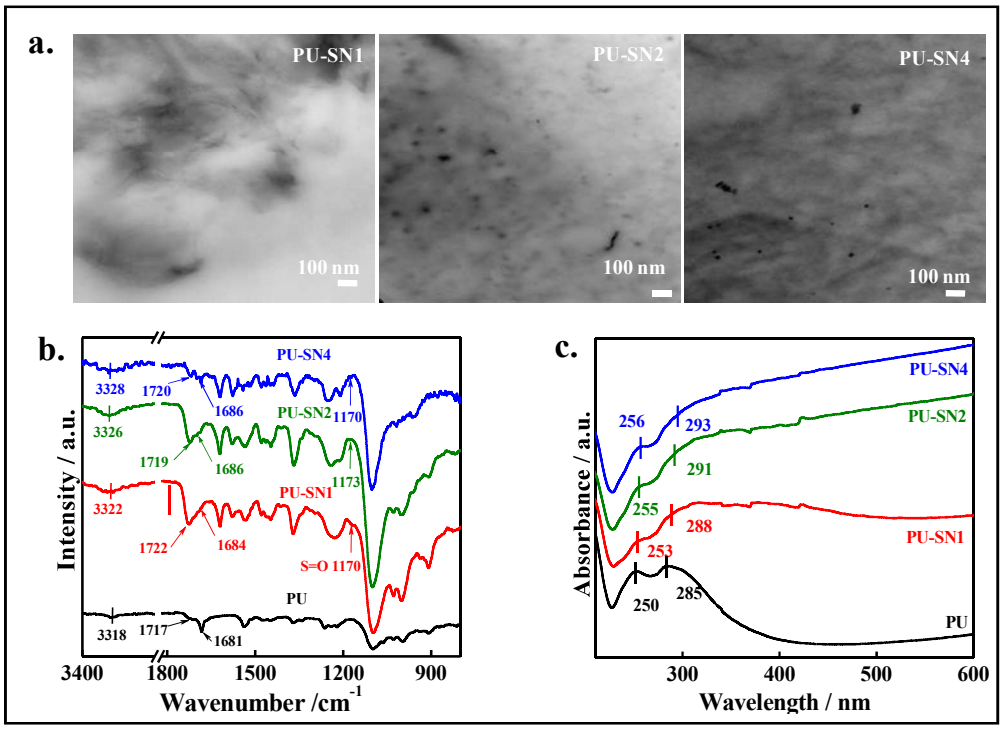

Figure 6.4: (a) Bright field Transmission electron micrographs of indicated nanocomposites, **(b)** FTIR and **(c)** UV-visible spectra of pure polyurethane and its indicated nanocomposites.

6.2.5 Structure and Morphology:

The variation of crystallinity in pure polymer and its nanocomposites is revealed through XRD measurement and it is given in (Figure 6.5a). Pure polyurethane exhibits sharp peaks at ~22.1^0 and ~23.9^0 indicating the crystalline nature due to the predominantly hydrogen bonding interaction between the urethane moiety in polymer chain while intensity of this peaks were reduced in nanocomposites suggesting the amorphous nature by minimization of the hydrogen bonding interaction through modified graphene sheet in urethane moiety as observed in FTIR spectra. However, modified graphene exhibits the crystalline (grainy) surface morphology as observed in

SEM image. Pure polyurethane exhibits the flake like surface morphology suggesting the crystalline behavior whereas, grain morphology gradually disappeared in nanocomposites and cloth like morphology is observed in nanocomposites indicating the amorphous nature as observed in XRD measurement (Figure 6.5b).

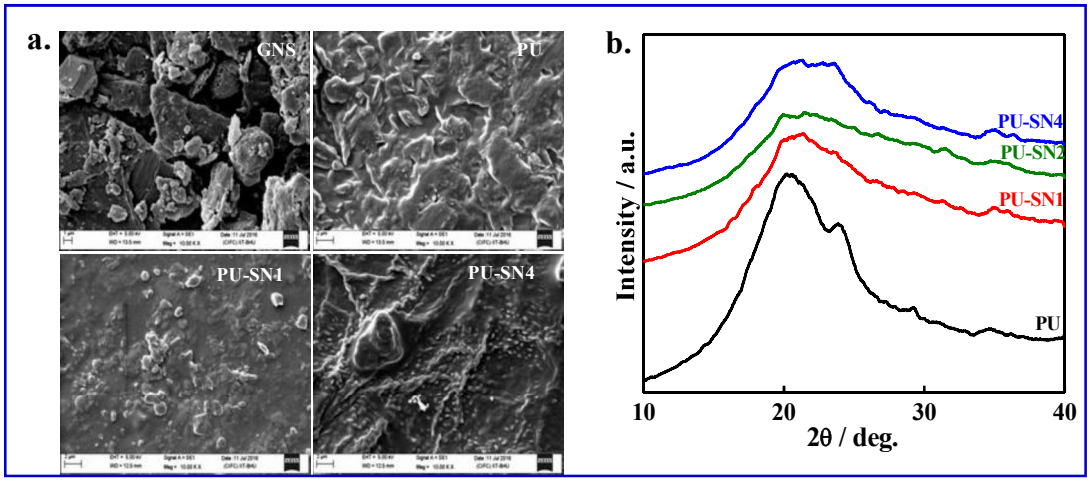

Figure 6.5: (a) SEM image modified graphene, pure PU and indicated nanocomposites, **(b)** XRD pattern of pure PU and indicated nanocomposites.

6.2.6 Graphene induced self-assembly in polyurethane:

The strips structure in aliphatic polyurethane as a consequence of hydrogen bonding interaction in urethane moiety cause the diffraction peak in XRD measurement. X-ray diffraction pattern of pure polyurethane and its indicated nanocomposites is given in (Figure 6.6a). Pure polyurethane exhibits a diffraction peak at 5.7^0 with corresponding d-spacing of 1.54nm indicating the presence of molecular sheet structure [Mishra et al. (2010)]. Shifting of peak position towards higher angle (lower d-spacing; 1.40nm) indicating the compact packing of the molecular sheet through the higher interaction in

nanocomposites. Furthermore, presence of hump patterns in small angle scattering measurement (SANS) (Figure 6.6b), at q~0.42nm^{-1} with corresponding to characteristic length, $\Lambda_c(=2\pi/q_m)$ of 15, 14.6, 11 and 10nm for pure PU, PU-SN1, PU-SN2 and PU-SN4 respectively. Decrease in characteristic value in nanocomposites as compared to pure polyurethane indicates the lesser number of molecular sheets are required to assemble for formation of domain pattern in nanocomposites. Therefore, self-assembly phenomena through the interaction which influence the properties are facilitated in presence of modified graphene. Lowering in characteristic length (Λ_c) in polyurethane graphene nanocomposites is also reported in our previous work [Patel et al. (2015)]. SANS patterns are best fitted in Ornstein-Zernike model (Equ.1).

$$I(q) = I(0) / (1+\xi^2 q^2)$$

Whereas, I(q) is the scattered intensity at peak maxima, I(0) is scattered intensity at zero wave vector, which value can obtained by the extra plotting the data, ξ is the correlation length and q is the wave vector. The correlation length (ξ) of pure PU, PU-SN1, PU-SN2 and PU-SN4 are 0.60, 1.37, 3.35and 3.75nm respectively. Ornstein-Zernike model for calculating the correlation length (ξ) is given in insight of SANS measurement. Correlation length (ξ) is the lateral dimension of domain structure form by the interaction and it is higher in nanocomposites as compared to pure PU. This is due to the presence of the modified graphene sheet in nanocomposites [Patel et al. (2016)]. Furthermore, higher order self-assembly through the interaction in pure polyurethane and its indicated nanocomposites is revealed through AFM measurement and given in (Figure 6.6c). Pure polyurethane exhibits the domain structure with

dimension of ~317nm in AFM image which becomes more prominent in order of ~687nm in nanocomposites due to the greater accumulation of the molecular sheet through interaction. Optical image also supports the higher order of self-assembled structure with dimension of ~3.1μm crystalline pattern in pure polymer which size gradually decreases in nanocomnposites (Figure 6.6d). The reason for formation of such self-assembled structure in pure aliphatic polyurethane is well reported and it is due to the extensive hydrogen bonding interaction in urethane moiety whereas in nanocomposites this is happened through the polar interaction between electron rich moiety of modified graphene sheet and dipole of urethane linkage [Patel et al. (2015); Mishra et al. (2010)]. Formation of nanostructure and step by step self-assembled is confirmed through the XRD measurement (1.54nm) with gradual increasing the molecular stack size in SANS (15nm) which form larger crystalline cluster of size ~317nm as observed in AFM image and subsequently more crystalline domain in (~3.1μm) in optical images.

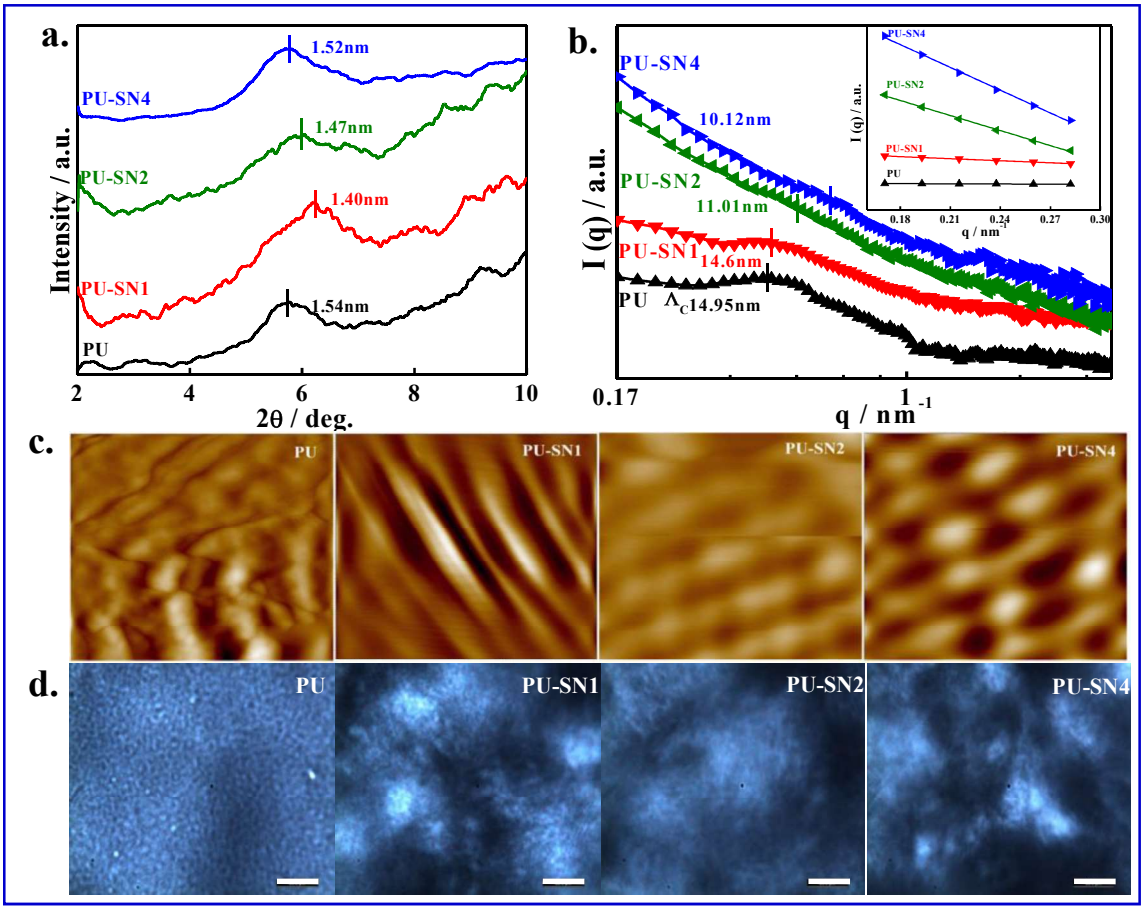

Figure 6.6: (a) X-ray diffraction patterns of PU and its indicated nanocomposites. Vertical lines indicate the peak position with interplanar spacing; **(b)** Small angle neutron scattering patterns; I (q) vs q (wave vector) plot of PU and its indicated nanocomposites. Inset figure shows the Ornstein-Zernike fitting for the calculation of correlation length, (ξ); **(c)** AFM images of PU and its indicated nanocompositess (1μm × 1μm) obtained through tapping mode **(d)** Optical images of PU and its indicated nanocomposites. (Scale bar 20 μm).

6.2.7 Gravimetric Measurement:

The weight loss of mild steel samples in 0.5M H_2SO_4 in absence and presence of sulfonated graphene, pure PU and 1% Nanocomposite was determined after 24h of immersion at 25^0C. The value of corrosion inhibition was calculated through following formula.

$$\%IE = \frac{W^0 - W}{W^0} \times 100$$

Where, W^0 and W are the weight loss of mild steel samples without and with the addition of the samples, respectively. Variation of %IE with different concentration of sulfonated graphene, pure PU and its nanocomposites are given in (Figure 6.7). It was clearly observed that rapid increase in IE was occurred in nanocomposites as compared to pure PU at lower concentration region (10ppm, ~65% IE) which further increased by increasing the concentration of nanocomposites. These increases in the IE in nanocomposites are due the presence of the active centre (ionic sulfonate group in graphene ring) which facilitates the adsorbability on the larger metal surface area and preventing the corrosion process in nanocomposite [Banerjee et al. (2011)]. Polyacrylic acid exhibits the maximum 77% IE at 280ppm level whereas, nanocomposite show the 78% IE at just 100ppm level which further enhanced to 90% IE at 200ppm indicating that developed material may have the potential to used a corrosion inhibitor [Amin et al. (2009)].

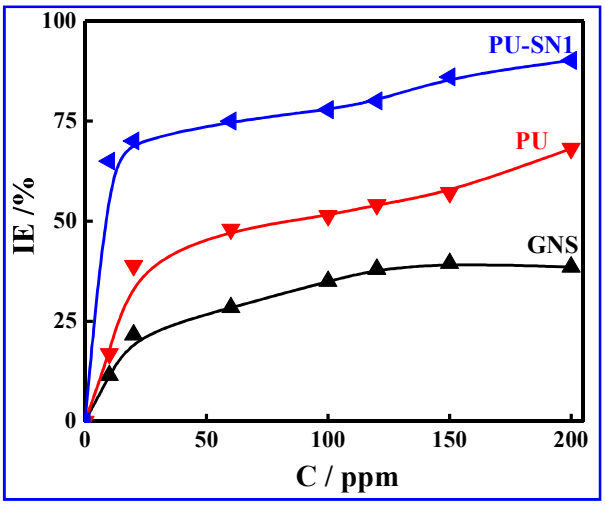

Figure 6.7: Corrosion inhibition efficiency of modified graphene, pure PU and indicated nanocomposite.

6.2.8 Biocompatibility Studies:

6.2.8.1 Cell Viability:

Biocompatible nature of pure polyurethane and its nanocomposites is evaluated through MTT assay using the HeLa cell lines in different time interval and has been given in (Figure 6.8a). Cells treated only through culture medium were treated as control. Cell viability of nanocomposites with lower content (1wt %) of sulfonated garphene was slightly higher than pure polyurethane at different time 1, 3 and 5days interval indicating the more biocompatible nature. Moreover, decrease in cell viability was observed in nanocomposites (2 and 4wt %) as compared to pure polyurethane indicating some cytotoxic property. Decrease in cell viability of nanocomposites with higher concentration of sulfonated graphene (2 and 4%wt.) is explained by grater interaction between the sulfonated graphene and insoluble formazan formed during MTT assay that stabilized this and suppressed to form the soluble formazan by addition of DMSO [Corr et al. (2013)]. Corr et al. (2013) were also studies the effect of the

sulfonated graphene on Hep3B cell lines and drastically decrease the cell viability was observed upto 20% at 100 μg/ml concentration and complete necrosis of cells were occurred at 72h interval [Corr et al. (2013)]. Moreover, nanocomposite with 4wt % of sulfonated graphene still showing the 60% cell viability after 5days interval suggesting that grafting of the biocompatible polyurethane chains with sulfonated graphene sheet through amine moiety induced the biocompatible nature in nanocomposites with even at higher content of sulfonated graphene. Cell viability data was further supported by the Fluorescence image of cell proliferation using acridine orange and ethydine bromide dye (Figure 6.8b). Cells were healthier on nanocomposite having the low content (1wt %) of sulfonated graphene compared to pure polyurethane and other nanocomposites. Furthermore, acceleration in cell (human mesenchymal stem cells) differentiation on the surface of graphene film has been also reported which depends upon the cell growth [Nayak et al. (2011)].

6.2.8.2 Cell Adhesion:

Polyurethane a well known biocompatible material is frequently used in medical arena as a transplant material [Hsu et al. (2010)]. Biocompatibility of pure polyurethane and its nanocomposites have been evaluated in term of cell adhesion on HeLa cell lines (Figure 6.8c). Nanocomposites having lower content of sulfonated graphene (1wt%) exhibits the better cell adhesion property compared to pure polyurethane which further decrease nanocomposites having higher content of sulfonated graphene (2 and 4wt %) indicating the biocompatible nature upto a certain concentration limit. Integrated Modulation Contrast (IMC) image of HeLa cell cultured

on pure polyurethane and its nanocomposites (Figure 6.8d) were also support the cell adhesion nature of material. Cells were more properly adhered on nanocomposites having 1wt % of sulfonated graphene as well as pure polyurethane. Alternation in cell morphology was observed in nanocomposites having the higher content ((2 and 4wt %) of sulfonated graphene suggesting the some toxic effect [Corr et al. (2013)]. In this view, it is suggested that 1wt % should be the upper concentration limit for sulfonated graphene to use as a fully biocompatible material.

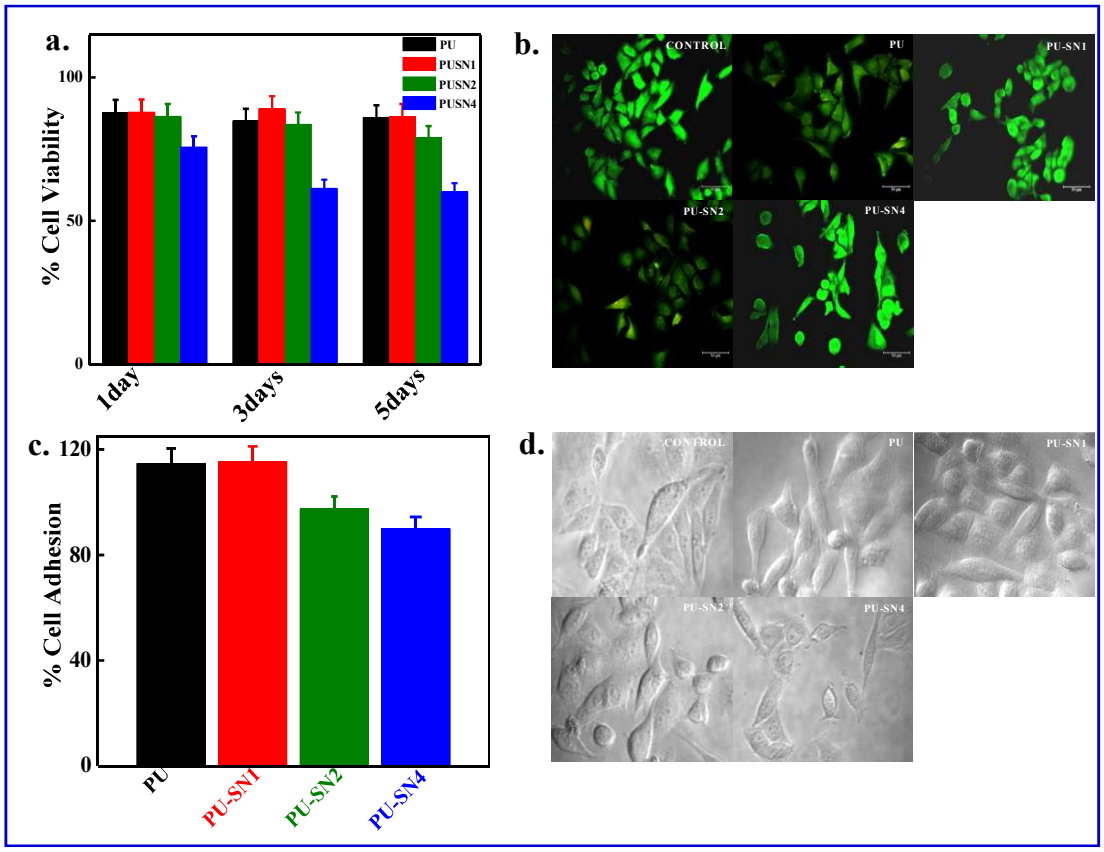

Figure 6.8: Biological behavior of pure PU and its indicated nanocomposites **(a)** Cell viability of pure PU and its indicated nanocomposites with time interval of 1, 3 and 5 days **(b)** Fluorescence microscopic image of PU and its indicated nanocomposites after 1 day of cell proliferation (Mag: 20×) and **(c)** Cell adhesion on pure PU and its indicated nanocomposites after 1day and **(d)** Integrated Modulation Contrast (IMC) mage of HeLa cell cultured on pure polyurethane and its nanocomposites after 24h (Mag: 40×)

6.3 Conclusion:

Properties of polymeric material are highly affected by the functionalization nature and dispersion of graphene in matrix. Sulfonation of graphene oxide is confirmed through FTIR and ^{1}H-NMR measurement. Grafting of prepolymer with modified graphene is revealed through FTIR and ^{1}H-NMR measurement. Self-assembly phenomena which play an important role in improvement of properties are also facilitated in presence of modified graphene. Nanocomposites exhibit the superior corrosion inhibition property as compared to pure polymer. Grafting of biocompatible prepolymer chain with sulfonated garphene leads to significant improvement in biocompatible nature of nanocomposites even at higher content. These results suggest that developed material may have the potential to use as a corrosive inhibitor and tissue engineering arena.